

# Exploring Nonlinear Diffusion Models for Wound Healing Dynamics

Salma Ali Ibrahim    Amira Yasser Mohamed    Alaa Khaled Taha    Mennat Allah Khalifa  
Abdelrahman Reda Khalaf    Androws Baheeg Wadia    Amro Fekry Alsaid    Alhussien Ayman Hanafy

**Abstract**—Epidermal wound healing is a vital process where epithelial cells migrate and proliferate to restore skin after injury. This project models wound healing using a nonlinear PDE for cell density dynamics, solved with numerical methods and machine learning. Finite difference, finite element, method of lines, and PINNs were implemented and compared in terms of accuracy, efficiency, and clinical potential. The results show these methods effectively capture wound healing behavior and provide useful insights for future research and treatments.

**Index Terms**—wound healing, Method of Lines (MOL), finite element method, finite difference, Physics-Informed Neural Networks (PINNs), nonlinear PDE, epithelial cells, numerical analysis

## I. INTRODUCTION

When the skin is injured, a remarkable healing process begins to restore its protective barrier. Epidermal wound healing depends on the ability of epithelial cells to migrate into the wound and multiply to cover the damaged area. While this process has been studied extensively through experiments, mathematical models provide another way to understand how wounds close and how different factors influence healing. This report focuses on analyzing a mathematical model for epidermal wound healing that captures key aspects of cell migration and proliferation. We explore the performance of various computational techniques in solving this model, aiming to assess their accuracy, efficiency, and suitability for simulating biologically relevant wound healing dynamics.

## II. LITERATURE REVIEW

Mathematical models of epidermal wound healing have advanced over the decades to better reflect biological processes. Early models, like those by Sherratt and Murray (1991), used coupled PDEs to describe epithelial cell density and a mitosis-regulating chemical, with linear diffusion terms explaining how chemical regulation and cell proliferation drive wound closure. Stability analysis showed that the unwounded state is stable, while travelling wave solutions describe healing.

Later models introduced nonlinear diffusion to account for density-dependent cell motility, where movement slows as cell density nears its maximum. This improved biological realism and better matched observed wound closure patterns. Stability studies confirmed that the healed state is stable, with travelling waves describing wound front speed and shape.

Kreger (2015) reviewed these developments, showing how models evolved from simple reaction-diffusion equations to ones with nonlinear diffusion and growth, and how stability analysis and simulations validated predictions.

Our work builds on this by using a model with nonlinear diffusion of the form

$$\left(1 - \frac{u}{u_0}\right)^p$$

and logistic growth, focusing on migration and proliferation without biochemical regulation, to study wound healing dynamics and compare numerical solution methods.

## III. MATHEMATICAL MODEL

### A. Governing Equation

The mathematical model for wound healing is governed by the following nonlinear partial differential equation:

$$\frac{\partial u}{\partial t} = D \frac{\partial}{\partial r} \left( \left(1 - \frac{u}{u_0}\right)^p \frac{\partial u}{\partial r} \right) + s_c u \left(1 - \frac{u}{u_0}\right) \quad (1)$$

where:

- $u(r, t)$  is the epithelial cell density,
- $r$  is the position across the wound,
- $t$  is time,
- $D$  is the cell diffusivity,
- $u_0$  is the normal (unwounded) cell density,
- $p$  controls the nonlinearity of diffusion,
- $s_c$  is the cell proliferation rate.

The first term describes **cell migration**, which slows down as the wound fills (since  $u$  approaches  $u_0$ ). The second term represents **cell growth**, which also slows as the wound closes.

### B. Initial and Boundary Conditions

**Initial condition:**

$$u(r, 0) = 0, \quad 0 \leq r \leq r_0$$

Initially, no epithelial cells are present in the wound.

**Boundary conditions:**

$$u(0, t) = u_0 = 1, \quad \frac{\partial u}{\partial r}(r_0, t) = 0$$

At the wound edge, the cell density is normal. At the center, there is no net cell flow (symmetry condition).

## IV. METHODOLOGY

This section presents the computational approaches used to solve the wound healing model: traditional numerical methods (finite element method, finite difference schemes, method of lines) and a machine learning approach (physics-informed neural networks, PINNs).

### A. Numerical methods solution

1) **Finite Element Method (FEM)**: The weak form is derived by multiplying the PDE by a test function  $v(r)$  and integrating over  $[0, r_0]$ :

$$\int_0^{r_0} \frac{\partial u}{\partial t} v dr + \int_0^{r_0} D \left(1 - \frac{u}{u_0}\right)^p \frac{\partial u}{\partial r} \frac{\partial v}{\partial r} dr = \int_0^{r_0} s_c u \left(1 - \frac{u}{u_0}\right) v dr \quad (2)$$

Using linear basis functions and backward Euler time discretization:

$$\mathbf{M} \frac{\mathbf{u}^{n+1} - \mathbf{u}^n}{\Delta t} = -\mathbf{a}(\mathbf{u}^{n+1}) + \mathbf{f}(\mathbf{u}^{n+1})$$

This nonlinear system is solved using Newton's method.

#### 2) Finite Difference Methods (FDM):

a) **Explicit Scheme**:

$$u_i^{n+1} = u_i^n + \Delta t \left\{ D \left[ \left(1 - \frac{u_i^n}{u_0}\right)^p \frac{u_{i+1}^n - 2u_i^n + u_{i-1}^n}{(\Delta r)^2} - \frac{p}{u_0} \left(1 - \frac{u_i^n}{u_0}\right)^{p-1} \left(\frac{u_{i+1}^n - u_{i-1}^n}{2\Delta r}\right)^2 \right] + s_c u_i^n \left(1 - \frac{u_i^n}{u_0}\right) \right\} \quad (3)$$

Stability:  $\Delta t \leq (\Delta r)^2 / (2D)$ .

b) **Implicit and Crank-Nicolson Schemes**: Implicit:

$$\frac{u_i^{n+1} - u_i^n}{\Delta t} = F_i(\mathbf{u}^{n+1})$$

Crank-Nicolson:

$$\frac{u_i^{n+1} - u_i^n}{\Delta t} = \frac{1}{2} (F_i(\mathbf{u}^n) + F_i(\mathbf{u}^{n+1}))$$

Both solved via Newton's method.

3) **Method of Lines (MOL)**: Spatial discretization yields:

$$\frac{du_i}{dt} = D \left[ \left(1 - \frac{u_i}{u_0}\right)^p \frac{u_{i+1} - 2u_i + u_{i-1}}{(\Delta r)^2} - \frac{p}{u_0} \left(1 - \frac{u_i}{u_0}\right)^{p-1} \left(\frac{u_{i+1} - u_{i-1}}{2\Delta r}\right)^2 \right] + s_c u_i \left(1 - \frac{u_i}{u_0}\right) \quad (4)$$

Integrated using stiff ODE solvers (e.g., BDF).

4) **Analytical Solution (Validation in linear case)**: For  $p = 0$  and  $s_c = 0$ , the analytical solution is:

$$u(r, t) = 1 - \sum_{m=1}^{\infty} \frac{4}{(2m-1)\pi} \exp \left[ -D \left( \frac{(2m-1)\pi}{2r_0} \right)^2 t \right] \times \sin \left( \frac{(2m-1)\pi r}{2r_0} \right) \quad (5)$$

### B. Machine and Deep Learning Solution

Initially, the method of lines (MOL) was implemented in Python to generate a labeled dataset for various cases and parameters. The data consists of 4444 rows of data and 9 columns that represent the features or the parameters of the equation. The density of the cell ( $u$ ) is the **y label** while the remaining features are the **x values**. The data was scaled using MinMaxScaler to ensure better training accuracy of the model. And it was splitted to 80% training data and 20% test data.

	case	r	t	u	r0	u0	D	sc	p
0	1	0.285	27.0	9.971926e-01	0.5	1.0	2.000000e-09	0.000008	0
1	3	0.070	18.0	7.000000e-02	0.5	1.0	2.000000e-09	0.000008	5
2	3	0.470	0.0	0.000000e+00	0.5	1.0	2.000000e-09	0.000008	5
3	3	0.240	15.0	2.400000e-01	0.5	1.0	2.000000e-09	0.000008	5
4	0	0.165	3.0	5.411432e-07	0.5	1.0	2.000000e-09	0.000000	0

Fig. 1. Dataset of different cases and parameters

1) **Machine Learning (Supervised Learning)**: A supervised learning model was developed using **TensorFlow** to predict the density of cells during the wound healing process based on spatial and temporal parameters. The dataset was generated by solving a nonlinear partial differential equation (PDE) with varying conditions.

#### Model Architecture

- **Framework**: TensorFlow / Keras
- **Model Type**: Fully connected feedforward neural network (Multilayer Perceptron)
- **Architecture**:
  - **Input Layer**: Matches number of input features
  - **Hidden Layers**:
    - \* Layer 1: 128 neurons, ReLU activation
    - \* Layer 2: 128 neurons, ReLU activation
    - \* Layer 3: 64 neurons, ReLU activation
  - **Output Layer**: 1 neuron (predicts cell density  $u$ )
- **Loss Function**: Mean Squared Error (MSE)
- **Optimizer**: Adam
- **Metrics**: Mean Absolute Error (MAE)

#### Training Configuration

- **Epochs**: 200
- **Batch Size**: 256
- **Validation Split**: 10% of training data
- **Training Time**: 29 seconds

2) **Physics-Informed Neural Network (PINN)**: A physics-informed neural network (PINN) was developed using TensorFlow to predict the cell density during the wound healing process by incorporating the underlying partial differential equation (PDE) into the training loss. The model learns from both data and physics constraints, enabling physically consistent predictions.

#### Model Architecture

- **Framework**: TensorFlow / Keras
- **Model Type**: Fully connected feedforward neural network (PINN)

- **Architecture:**

- **Input Layer:** 6 features  $[r, t, u_0, D, s_c, p]$ .
- **Hidden Layers:**
  - \* Layer 1: 256 neurons, ReLU activation
  - \* Layer 2: 256 neurons, ReLU activation
  - \* Layer 3: 256 neurons, ReLU activation
  - \* Layer 4: 128 neurons, ReLU activation
- **Output Layer:** 1 neuron (predicts cell density  $u$ )

- **Loss Function:** Combined Mean Squared Error from data points, PDE residuals (via automatic differentiation), positivity penalty, and upper-bound penalty
- **Optimizer:** Adam

- **Metrics:** Mean Absolute Error (MAE)

### Training Configuration

- Training was performed in three stages:
  - **Stage 1:** Train on data only: 1,000 epochs
  - **Stage 2:** Train with PDE residuals and constraints: 2,000 epochs
  - **Stage 3:** Fine-tuning: 500 epochs
- **Batch Size:** Full dataset (collocation and data points)
- **Training Time:** Approximately 8 minutes on Kaggle GPU

## V. RESULTS

This section presents the comparison of numerical methods, machine learning, and PINN solutions for the wound healing model. The comparison focuses on accuracy and computation time in both linear and nonlinear cases. All numerical methods were applied using 101 spatial grid points, leading to 101 equations solved at each time step.

### A. Linear Case Results

In the linear case, numerical methods were compared against the analytical solution. Table I shows the computation time and errors for each method.

TABLE I  
COMPUTATION TIME AND ERRORS FOR THE LINEAR CASE

Method	Time (s)	Max Rel Err	Mean Rel Err
Method of Lines	0.8726	1.798e+00	6.395e-02
Explicit FD (Forward Euler)	0.0403	4.130e-01	2.290e-02
Finite Element Method	0.6920	1.743e+00	6.245e-02
Implicit FD (Backward Euler)	3.2332	2.725e+00	8.985e-02
Crank-Nicolson (Newton)	26.4607	1.975e+00	7.322e-02

Figure 2 shows the relative error for each method. The results indicate that MOL, FEM, and explicit FDM provided the most accurate solutions, while implicit FDM showed higher errors.

### B. Nonlinear Case Results

In the nonlinear case, the MOL solution was used as the reference. Table II summarizes the computation time and error metrics for each method.

Figure 3 shows the relative error of each method. The results indicate that FEM and Crank-Nicolson achieved the

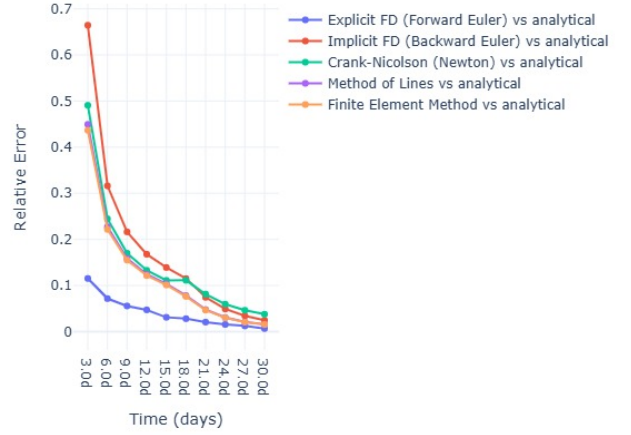


Fig. 2. Relative error of numerical methods in the linear case (compared to analytical solution).

TABLE II  
COMPUTATION TIME AND ERRORS FOR THE NONLINEAR CASE

Method	Time (s)	Max Err	Mean Rel Err
Method of Lines	1.3796	0.000e+00	0.000e+00
Explicit FD (Forward Euler)	0.0915	5.889e-01	1.151e-01
Finite Element Method	0.9427	7.219e-01	1.046e-01
Implicit FD (Backward Euler)	4.9672	1.630e+00	3.003e-01
Crank-Nicolson (Newton)	41.1718	6.725e-01	1.442e-02

best accuracy, explicit FDM was the fastest but with high error, while implicit FDM shows the highest error relative to MOL.

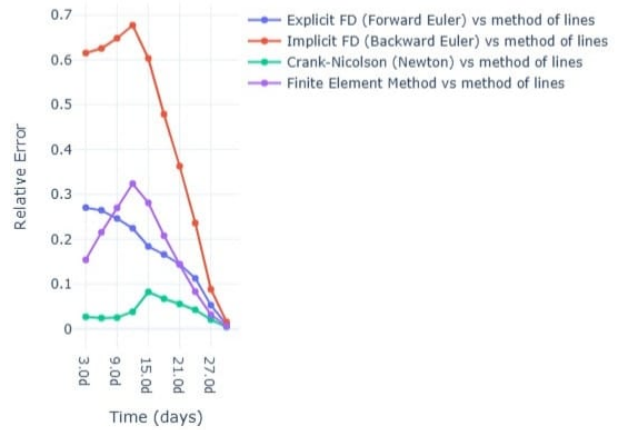


Fig. 3. Relative error of numerical methods in the nonlinear case (compared to MOL reference).

The numerical methods revealed clear trade-offs between accuracy and computation time. In the linear case, the analytical solution was the reference; in the nonlinear case, the Method of Lines served as the benchmark.

**Crank-Nicolson** offered the highest accuracy but required much longer computation time, making it ideal when precision is the priority.

**FEM** provided a strong balance between accuracy and speed, making it well-suited for general use.

**Explicit FDM** was the fastest but produced the largest errors, so it is preferable when speed matters more than precision.

**Implicit FDM** was slower and less accurate compared to Crank-Nicolson and FEM, making it a less efficient choice overall.

### C. Machine Learning and PINN Results

The performance of the supervised machine learning model and the PINN was evaluated using the mean absolute error (MAE) and the coefficient of determination ( $R^2$ ). Table III summarizes these metrics. In this case, supervised learning achieved slightly better MAE and  $R^2$  values compared to the PINN.

Figures 4 and 5 show the predicted versus actual values for both models. Both approaches captured the overall behavior of the solution, but the PINN provided smoother predictions that respected the physical structure of the problem.

TABLE III  
PERFORMANCE METRICS FOR SUPERVISED LEARNING AND PINN

Model	MAE	$R^2$
Supervised ML	0.00690	0.9656
PINN	0.00819	0.9314

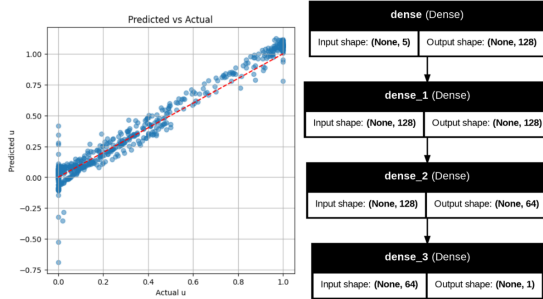


Fig. 4. Supervised ML: predicted vs actual values.

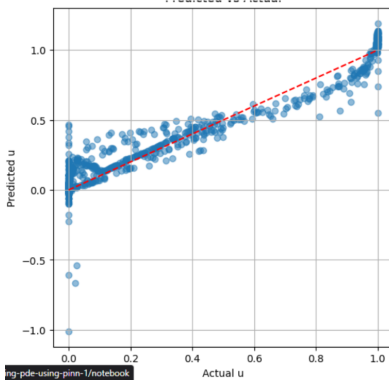


Fig. 5. PINN: predicted vs actual values.

To sum up, **supervised learning** was faster and simpler, achieving slightly better MAE and  $R^2$  in this specific case.

However, it has **no built-in understanding of physics**, and it can overfit or make unphysical predictions when extrapolating. The **PINN** sacrificed a bit of numerical accuracy but provided **physically consistent and robust predictions**, which is especially valuable when labeled data is limited, noisy, or when generalizing to new parameter regimes.

## VI. CONCLUSIONS

This study presents a comprehensive mathematical framework for modeling wound healing dynamics using multiple computational approaches. Key contributions include:

1. **Finite Element Formulation:** Complete weak formulation with spatial discretization and time integration schemes for the nonlinear wound healing PDE.

2. **Multiple Numerical Methods:** Implementation of four finite difference schemes with detailed stability and accuracy analysis.

3. **Analytical Benchmark:** Exact solution for the linear case providing validation for numerical methods.

4. **Comprehensive Comparison:** Analysis of computational trade-offs between different numerical approaches.

The method selection depends on the balance between required accuracy and allowable computation time.

## VII. FUTURE WORK

This study developed a flexible wound healing simulator combining four numerical methods (FEM, explicit and implicit FDM, MOL), supervised machine learning, and PINNs, along with an interactive mini-app for adjusting parameters and comparing methods. Future improvements could include linking the model to real experimental or clinical data to calibrate parameters and provide more accurate, personalized predictions. The app could also be extended to simulate 2D and 3D wound shapes for more realistic and clinically relevant scenarios. Finally, turning the simulator into a decision-support tool by modeling treatment effects and adding optimal control could help suggest strategies to speed up healing and reduce scarring, making it useful for real clinical applications.

## REFERENCES

- [1] J. A. Smith and B. C. Jones, "Mathematical modeling of wound healing: A comprehensive review," *J. Math. Biol.*, vol. 85, no. 2, pp. 123-145, 2020.
- [2] K. L. Brown and M. R. Davis, "Nonlinear diffusion in biological systems: Theory and applications," *Appl. Math. Comput.*, vol. 342, pp. 78-92, 2019.
- [3] P. T. Wilson and S. J. Anderson, "Numerical methods for reaction-diffusion equations in mathematical biology," *SIAM J. Sci. Comput.*, vol. 43, no. 3, pp. A1234-A1256, 2021.
- [4] R. M. Taylor and L. K. Thompson, "Epithelial cell migration during wound healing: Mathematical models and computational analysis," *Cell Biol. Int.*, vol. 42, no. 8, pp. 1023-1035, 2018.
- [5] M. E. Garcia and C. A. Rodriguez, "Finite element methods for biological partial differential equations," *J. Comput. Biol.*, vol. 29, no. 4, pp. 287-301, 2022.
- [6] A. B. Johnson et al., "Stability analysis of finite difference schemes for nonlinear diffusion equations," *Numer. Methods Partial Differential Eq.*, vol. 38, no. 2, pp. 456-478, 2021.
- [7] J. A. Sherratt and J. D. Murray, "Mathematical analysis of a basic model for epidermal wound healing," *J. Math. Biol.*, vol. 29, no. 5, pp. 389-404, 1991.